

Perturbation Theory for a Repulsive Hubbard Model in Quasi-One-Dimensional Superconductors

Sotaro SASAKI Hiroaki IKEDA and Kosaku YAMADA

Department of Physics, Kyoto University, Sakyo-ku, Kyoto 606-8502

(Received December 22, 2003)

We investigate pairing symmetry and transition temperature in a quasi-one-dimensional repulsive Hubbard model. We solve the Eliashberg equation using the third-order perturbation expansion with respect to the on-site repulsion U . We find that when the electron number density is shifted from the half-filled state, a transition into unconventional superconductivity is expected. When one-dimensionality is weak, a spin-singlet state is favorable. In contrast, when one-dimensionality is strong and electron number density is far from the half-filled state, a spin-triplet state is stabilized. Finally, we discuss the possibility of unconventional superconductivity caused by the on-site Coulomb repulsion in $\beta\text{-Na}_{0.33}\text{V}_2\text{O}_5$.

KEYWORDS: quasi-one-dimensional superconductors, pairing symmetry, transition temperature, third-order perturbation theory

Superconductivity in quasi-one-dimensional conductors has been studied as an important phenomenon. Today, some quasi-one-dimensional superconductors, such as $(\text{TMTSF})_2\text{X}^{1,2}$ and $\text{Sr}_{14-x}\text{Ca}_x\text{Cu}_{24}\text{O}_{41}$,³ have been discovered, and their superconductivity has been investigated. Recently, a superconducting transition in $\beta\text{-Na}_{0.33}\text{V}_2\text{O}_5$, which has a quasi-one-dimensional lattice structure similar to $\text{Sr}_{14-x}\text{Ca}_x\text{Cu}_{24}\text{O}_{41}$, has been discovered,⁴ and this phenomenon has attracted our attention. The transition temperature is $T_c \simeq 8$ K under high pressures of approximately 8 GPa. At ambient pressure, this material shows quasi-one-dimensional metallic behavior in an electric resistivity experiment at high temperature,⁵ and encounters a charge-ordered transition at $T_{\text{CO}} \simeq 135$ K.⁵ Furthermore, below $T_N \simeq 25$ K, an antiferromagnetic ordered phase appears in the charge-ordered phase.⁶ Under high pressures of approximately 8 GPa, the charge-ordered phase abruptly vanishes, accompanied by the superconducting transition.⁴ It is not clear under high pressure whether the antiferromagnetic phase in the charge-ordered phase survives or not. However, the existence of the antiferromagnetic phase at ambient pressure suggests that the electron correlation is important.

Such an electron correlation effect leads to unconventional superconductivity rather than conventional s-wave superconductivity induced by the electron-phonon coupling.⁷ Such investigations have already been reported in the quasi-one-dimensional superconductors, $(\text{TMTSF})_2\text{X}$ and $\text{Sr}_{14-x}\text{Ca}_x\text{Cu}_{24}\text{O}_{41}$. The superconductivity in $(\text{TMTSF})_2\text{X}$ has been investigated using the fluctuation-exchange approximation (FLEX)⁸ and the third-order perturbation theory (TOPT).⁹ Both theoretical calculations suggest that a d-wave like spin-singlet state is the most stable. Also, in $\text{Sr}_{14-x}\text{Ca}_x\text{Cu}_{24}\text{O}_{41}$, the FLEX calculation for the trellis lattice indicated a d-wave like spin-singlet state.¹⁰ However, experimentally, in both materials, the Knight shift does not change above and below T_c , and the spin-triplet state is indicated,^{11,12} although it is still confusing. Thus, intensive investigations on quasi-one-dimensional superconductors

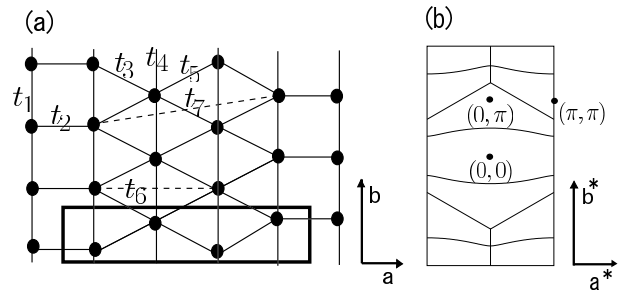


Fig. 1. (a) Schematic figure of the lattice used in this calculation. t_i ($1 \leq i \leq 7$) is the hopping integral. The region enclosed by rectangle is primitive cell. The primitive cell topologically composes triangular lattice. (b) The Fermi surface for $n = 0.90$, $t_0 = 1.0$. Since the lattice is topologically triangular lattice, the Brillouin zone is hexagonal.

should be carried out. In this letter, we investigate in detail unconventional superconductivity in a quasi-one-dimensional Hubbard model, taking up the superconductivity in $\beta\text{-Na}_{0.33}\text{V}_2\text{O}_5$.

Now, let us consider the lattice structure and the band structure in $\beta\text{-Na}_{0.33}\text{V}_2\text{O}_5$. This material has three types of vanadium site, V1, V2 and V3. V1 is on the VO_6 zigzag chain, V2 is on the VO_6 ladder chain and V3 is on the VO_5 zigzag chain. At ambient pressure, NMR experiments indicated that V3 does not have any conduction electrons at low temperatures.¹³ Assuming that conduction electrons at V3 are also empty under high pressures, we can consider the lattice structure with the V network shown in Fig. 1(a), which is important for electric conductivity. This structure is different from the trellis lattice only in the V1 zigzag chain in the middle of Fig. 1(a). The unit cell is a thick-line rectangle, and contains four V sites. Since there is no information on the band structure of $\beta\text{-Na}_{0.33}\text{V}_2\text{O}_5$, we discuss a simple tight-binding model with an s orbital on each V site. In this case, we consider 7 types of hopping integrals ($t_1 \sim t_7$) displayed in Fig. 1(a). By numerically diagonalizing the energy matrix, we obtain four bands, since

there are four orbitals in the unit cell. Among them, we only use the lowest energy band. In $\beta\text{-Na}_{0.33}\text{V}_2\text{O}_5$, there is one electron per unit cell, if we simply count the valence electrons. Under the ideal condition that all electrons occupy only the lowest energy band, it becomes half-filled. Therefore, we deal with the electron number density n as a parameter less than the half-filled state. If the superconductivity of this material is caused by electron correlation, electron correlation must be strong. For electron correlation to be strong, a high-density band is required. Therefore, the electrons should mainly occupy the lowest energy band. From these viewpoints, we use the single-band model. If there is no high-density band, we have to consider a mechanism other than electron correlation. As a typical set of parameters, we use $t_1 = 1.0$, $t_2 = t_0$, $t_3 = t_4 = t_5 = 0.3t_0$ and $t_6 = t_7 = 0.2t_0$. Here, t_0 is a measure of one-dimensionality, and with decreasing t_0 , the Fermi surface becomes more one-dimensional. We assume that the results of calculations mainly depend on the one-dimensionality of the Fermi surface. Actually, when we change the ratio of the transfer integrals t_i maintaining the one-dimensionality of the Fermi surface, the results of the calculations are almost unchanged. Therefore, we can study the dependence of the form of the Fermi surface using the parameter t_0 . In Fig. 1(b), we show a typical quasi-one-dimensional Fermi surface for $t_0 = 1.0$ and the electron number density $n = 0.90$. This Fermi surface possesses a less nesting property, and is different from the band structures with an almost perfect nesting property discussed so far in the quasi-one-dimensional model calculations. Here, we investigate in detail superconductivity in such a situation. We consider the quasi-one-dimensional single-band Hubbard model with the lowest band $\varepsilon(k)$ discussed above,

$$H = \sum_{k,\sigma} \varepsilon(k) c_{k\sigma}^\dagger c_{k\sigma} + \frac{U}{2N} \sum_{k_i} \sum_{\sigma \neq \sigma'} c_{k_1\sigma}^\dagger c_{k_2\sigma'}^\dagger c_{k_3\sigma'} c_{k_4\sigma} \delta_{k_1+k_2, k_3+k_4}. \quad (1)$$

We treat this model using the third-order perturbation expansion. Hereafter, in order to obtain a moderate transition temperature T_c , we set $U = 5.0$, which is almost equal to the bandwidth. The third-order perturbation theory in the strongly correlated region has been justified by higher-order calculations of pairing interactions.¹⁴ We can apply the perturbation theory for the appropriate values of U to obtain the reliable value of T_c .

We apply the third-order perturbation theory with respect to U to our model. Diagrams of the normal self-energy are shown in Fig. 2. The normal self-energy is given by

$$\Sigma_N(k) = \frac{T}{N} \sum_{k'} [U^2 \chi_0(k-k') G_0(k')] + U^3 (\chi_0^2(k-k') + \phi_0^2(k+k')) G_0(k'), \quad (2)$$

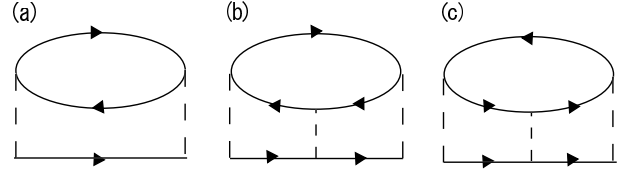


Fig. 2. The diagrams of Normal self-energy. The solid lines represent Green's function $G_0(k)$ and the broken lines represent the Coulomb repulsion U .

where

$$G_0(k) = \frac{1}{i\omega_n - \varepsilon(\mathbf{k}) + \mu},$$

$$\chi_0(q) = -\frac{T}{N} \sum_k G_0(k) G_0(q+k), \quad (3)$$

$$\phi_0(q) = -\frac{T}{N} \sum_k G_0(k) G_0(q-k).$$

Here, $G_0(k)$ with the short notation $k = (\mathbf{k}, \omega_n)$ represents the bare Green's function. Since the first-order normal self-energy is constant, it can be included by the chemical potential μ . The dressed Green's function $G(k)$ is given by

$$G(k) = \frac{1}{i\omega_n - \varepsilon(\mathbf{k}) - \Sigma_N(k) + \mu + \delta\mu}. \quad (4)$$

Here, the chemical potential μ and the chemical potential shift $\delta\mu$ are determined so as to fix the electron number density n ,

$$n = 2 \frac{T}{N} \sum_k G_0(k) = 2 \frac{T}{N} \sum_k G(k). \quad (5)$$

We also expand the effective pairing interaction up to the third order with respect to U . For the spin-singlet state, the effective pairing interaction is given by

$$V^{\text{Singlet}}(k; k') = V_{\text{RPA}}^{\text{Singlet}}(k; k') + V_{\text{Vertex}}^{\text{Singlet}}(k; k'), \quad (6)$$

where

$$V_{\text{RPA}}^{\text{Singlet}}(k; k') = U + U^2 \chi_0(k-k') + 2U^3 \chi_0^2(k-k'), \quad (7)$$

and

$$V_{\text{Vertex}}^{\text{Singlet}}(k; k') = 2(T/N) \text{Re} \left[\sum_{k_1} G_0(k_1) \times (\chi_0(k+k_1) - \phi_0(k+k_1)) G_0(k+k_1-k') U^3 \right]. \quad (8)$$

For the spin-triplet state,

$$V^{\text{Triplet}}(k; k') = V_{\text{RPA}}^{\text{Triplet}}(k; k') + V_{\text{Vertex}}^{\text{Triplet}}(k; k'), \quad (9)$$

where

$$V_{\text{RPA}}^{\text{Triplet}}(k; k') = -U^2 \chi_0(k-k'), \quad (10)$$

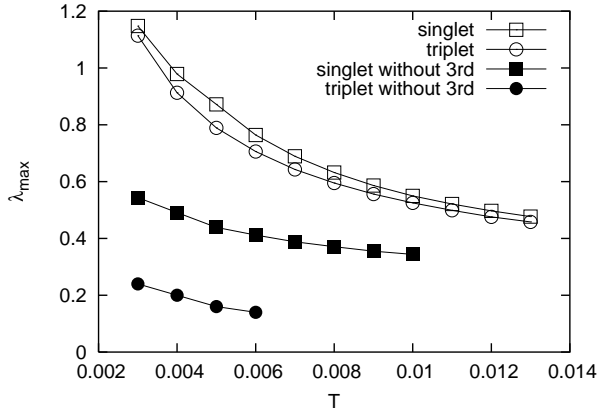


Fig. 3. Calculated maximum eigenvalues λ_{\max} for spin-singlet (or spin-triplet) state. The line with white squares (circles) is the result for the spin-singlet (spin-triplet) state obtained using the third-order perturbation theory. The line with the black squares (circles) is the result for the spin-singlet (spin-triplet) state without the pairing interaction due to the third-order terms. The parameters are $n = 0.90$ and $t_0 = 1.0$.

and

$$V_{\text{Vertex}}^{\text{Triplet}}(k; k') = 2(T/N) \text{Re} \left[\sum_{k_1} G_0(k_1) \right. \\ \left. \times (\chi_0(k+k_1) + \phi_0(k+k_1)) G_0(k+k_1-k') U^3 \right]. \quad (11)$$

Here, $V_{\text{RPA}}^{\text{Singlet(Triplet)}}(k, k')$ is called the RPA terms and $V_{\text{Vertex}}^{\text{Singlet(Triplet)}}(k, k')$ is called the vertex corrections. Near the transition point, the anomalous self-energy $\Delta(k)$ satisfies the linearized Eliashberg equation,

$$\lambda_{\max} \Delta(k) = -\frac{T}{N} \sum_{k'} V(k; k') |G(k')|^2 \Delta(k'), \quad (12)$$

where, $V(k; k')$ is $V^{\text{Singlet}}(k; k')$ or $V^{\text{Triplet}}(k; k')$, and λ_{\max} is the largest positive eigenvalue. Then, the temperature at $\lambda_{\max} = 1$ corresponds to T_c . By estimating λ_{\max} , we can determine which type of pairing symmetry is stable. For numerical calculations, we take 128×128 \mathbf{k} -meshes for twice space of the first Brillouin zone and 2048 Matsubara frequencies.

In Fig. 3, we show the results for λ_{\max} in the case with $n = 0.90$ and $t_0 = 1.0$. With decreasing temperature, λ_{\max} increases. The spin-singlet state and the spin-triplet state possess almost the same transition temperature, $T_c \simeq 0.004$. If we assume that the bandwidth $W \simeq 5$ corresponds to 1 eV, then $T_c \simeq 8$ K is obtained in accordance with the experimental value for $\beta\text{-Na}_{0.33}\text{V}_2\text{O}_5$. In Fig. 3, we also show the results for λ_{\max} obtained without the pairing interaction due to the third-order terms. For the spin-triplet state, we see that the vertex corrections are important for stabilizing the spin-triplet state from the comparison.

In Fig. 4, we show the momentum dependence of $\chi_0(\mathbf{q}, 0)$ and $\phi_0(\mathbf{q}, 0)$ in the case with $n = 0.90$, $t_0 = 1.0$ and $T = 0.004$. Since the Fermi surface has a nesting property, $\chi_0(\mathbf{q}, 0)$ has peaks near $\mathbf{q} = (\pi, \pi)$ and $\mathbf{q} = (0, \pi)$. Since the Brillouin zone is hexagonal, (π, π)

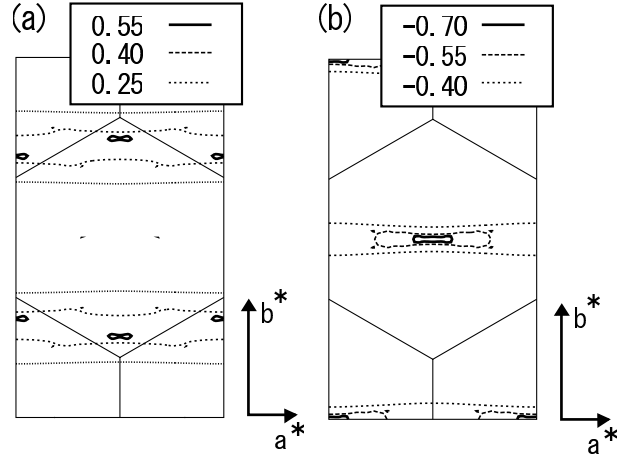


Fig. 4. (a) Contour plots of $\chi_0(\mathbf{q}, 0)$. The peaks exist near $\mathbf{q} = (\pi, \pi)$ and $\mathbf{q} = (0, \pi)$ (b) Contour plots of $\phi_0(\mathbf{q}, 0)$. The peaks exist at $\mathbf{q} = (0, 0)$. The parameters are $n = 0.90$, $t_0 = 1.0$ and $T = 0.004$.

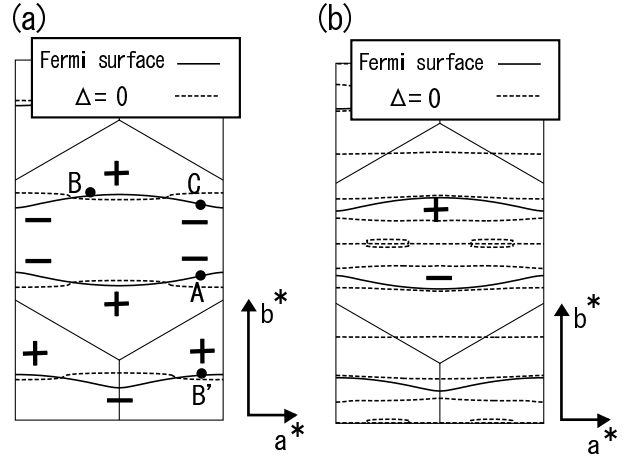


Fig. 5. (a) Contour plot of the anomalous self-energy. $\Delta(k) = 0$ for the spin-singlet state has d-wave like momentum dependence. (b) Contour plot of the anomalous self-energy. $\Delta(k) = 0$ for the spin-triplet state has p-wave like momentum dependence. The parameters are $n = 0.90$, $t_0 = 1.0$ and $T = 0.01$.

is equivalent to $(0, \pi)$. At the half-filled state, $\chi_0(\mathbf{q}, 0)$ has peaks beside $\mathbf{q} = (\pi, \pi)$ and $\mathbf{q} = (0, \pi)$. If the electron number density n is shifted from the half-filled state, then the peaks are shifted from $\mathbf{q} = (\pi, \pi)$ and $\mathbf{q} = (0, \pi)$. On the other hand, $\phi_0(\mathbf{q}, 0)$ has a peak at $\mathbf{q} = (0, 0)$.

In Fig. 5, we show the contour plots of the anomalous self-energy in the case of $n = 0.90$, $t_0 = 1.0$ and $T = 0.01$. For the spin-singlet state, the momentum dependence of the anomalous self-energy on the Fermi surface is a d-wave like state with node. For the spin-triplet state, the momentum dependence of the anomalous self-energy is p-wave like, and is a fully gapped state. For the spin-singlet state, the RPA terms are dominant in the effective interaction terms. In this case, we can easily understand the gap structure in Fig. 5(a) from the structure in the Eliashberg equation as follows. The peak structures of $\chi_0(\mathbf{q}, 0)$ in Fig. 4(a) originate from the nesting property, between around point A and around point B, or around

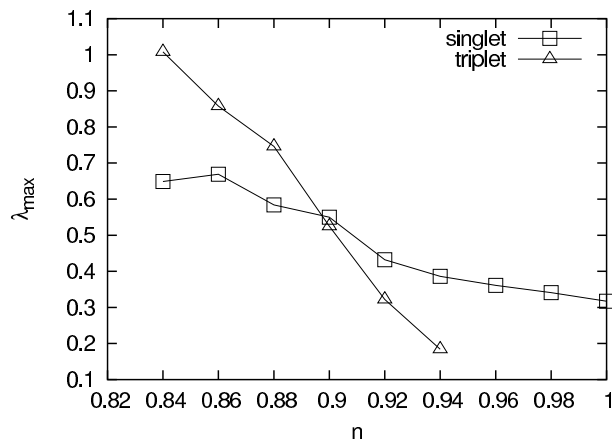


Fig. 6. λ_{\max} as a function of n . The parameters are $T = 0.01$ and $t_0 = 1.0$.

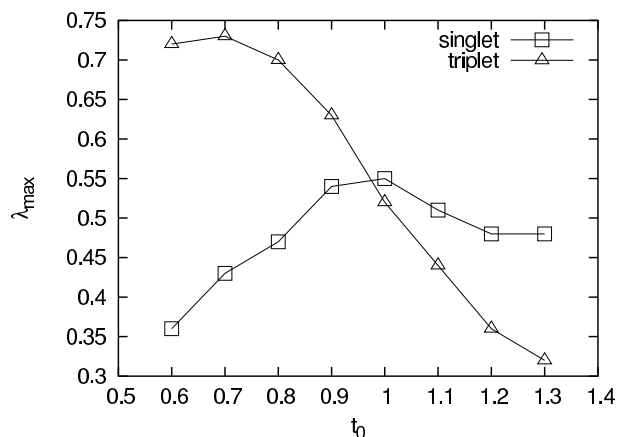


Fig. 7. λ_{\max} as a function of t_0 . The parameters are $n = 0.90$ and $T = 0.01$.

point B' on the Fermi surfaces in Fig. 5(a). In order to obtain a positive value of λ_{\max} , it is favorable that signs of $\Delta(k)$ around points B and B' are different from its sign around point A. The structure of $\Delta(k)$ in Fig. 5(a) just becomes so.

In Fig. 6, n dependence of λ_{\max} is shown. If n is near the half-filled state, the spin-singlet and the spin-triplet states have low values of λ_{\max} . With decreasing n , λ_{\max} increases, and the spin-singlet and spin-triplet states yield nearly the same λ_{\max} at $n \simeq 0.90$. Moreover, with decreasing n from $n = 0.90$, the values of λ_{\max} for the spin-triplet state become larger than those for the spin-singlet state. This indicates that the spin-triplet state may be realized far from the half-filled state. We can easily understand why the values of λ_{\max} are suppressed for the spin-singlet and spin-triplet states at around the half-filled state. For spin-singlet state, at the half-filled state, $\chi_0(\mathbf{q}, 0)$ has a peak beside $\mathbf{q} = (0, \pi)$. Considering the structure of the Eliashberg equation, in order to obtain a large positive value of λ_{\max} , it is not favorable that signs of $\Delta(k)$ around point A are the same as its sign around point C on the Fermi surface in Fig. 5(a). Therefore, the values of λ_{\max} are strongly suppressed around the half-filled state by the conflicting

peaks of $\chi_0(\mathbf{q}, 0)$. On the other hand, if the electron number density is far from the half-filled state, the peak of $\chi_0(\mathbf{q}, 0)$ is far from $\mathbf{q} = (0, \pi)$. Therefore, the suppression of the values of λ_{\max} becomes weak. For the spin-triplet state, when the Fermi surface has perfect particle-hole symmetry, the vertex corrections are perfectly canceled out, and at approximately the half-filled state, owing to approximate particle-hole symmetry, vertex corrections are approximately canceled out and the values of λ_{\max} are suppressed. Here, the normal self-energy term corresponding to Fig. 2(c) make the mass enhancement factor small. When the Fermi surface have perfect particle-hole symmetry, the terms corresponding to Figs. 2(b) and 2(c) are perfectly canceled out. However, for $n \leq 0.82$, particle-hole symmetry deteriorates, and the mass enhancement factor is much smaller than unity. Therefore, reliable numerical calculation cannot be obtained in the range of $n \leq 0.82$.

In Fig. 7 we show the t_0 dependence of λ_{\max} . With decreasing t_0 , the spin-triplet state becomes dominant, and with increasing t_0 , the spin-singlet state becomes dominant. If t_0 is small, $\chi_0(\mathbf{q}, 0)$ have the character of one-dimensionality. In this case, the values of λ_{\max} are suppressed by the conflict of the peaks of $\chi_0(\mathbf{q}, 0)$ like the above case.

In conclusion, we have investigated pairing symmetry and the transition temperature on the basis of a quasi-one-dimensional Hubbard model. We have solved the Eliashberg equation using the third-order perturbation theory with respect to the on-site repulsion U . We find that if n is shifted from the half-filled state, the transitions into unconventional superconductivity is expected. If one-dimensionality is weak, a spin-singlet pairing is more stable than a spin-triplet one. In contrast, if one-dimensionality is strong and n is far from the half-filled state, a spin-triplet pairing is more stable than a spin-singlet one. Thus, we suggest the possibility of unconventional superconductivity in $\beta\text{-Na}_{0.33}\text{V}_2\text{O}_5$ caused by the on-site Coulomb repulsion.

Numerical calculation in this work was carried out at the Yukawa Institute Computer Facility.

- 1) For review, T. Ishiguro, K. Yamaji and G. Saito: *Organic Superconductors* (Springer-Verlag, Heiderberg, 1998)
- 2) D. Jérôme and H. J. Schulz: *Adv. Phys.* **31** (1982) 299.
- 3) M. Uehara, T. Nagata, J. Akimitsu, H. Takahashi, N. Mōri and K. Kinoshita: *J. Phys. Soc. Jpn.* **65** (1996) 2764.
- 4) T. Yamauchi, Y. Ueda and N. Mōri: *Phys. Rev. Lett.* **89** (2002) 057002.
- 5) H. Yamada and Y. Ueda: *J. Phys. Soc. Jpn.* **68** (1999) 2735.
- 6) Y. Ueda: *J. Phys. Soc. Jpn.* **69** (2000) Suppl. B. pp. 149.
- 7) Y. Yanase, T. Jujo, T. Nomura, H. Ikeda, T. Hotta, K. Yamada: *Phys. Rep.* **387** (2003) 1.
- 8) H. Kino and H. Kontani: *J. Phys. Soc. Jpn.* **68** (1999) 1481.
- 9) T. Nomura and K. Yamada: *J. Phys. Soc. Jpn.* **70** (2001) 2694.
- 10) H. Kontani and K. Ueda: *Phys. Rev. Lett.* **80** (1998) 5619.
- 11) I. J. Lee *et al.*: *Phys. Rev. B* **68** (2003) 092510.
- 12) N. Fujiwara, N. Mōri, Y. Uwatoko, T. Matsumoto, N. Motoyama and S. Uchida: *Phys. Rev. Lett.* **90** (2003) 137001.
- 13) M. Itoh, N. Akimoto, H. Yamada, M. Isobe and Y. Ueda: *J. Phys. Soc. Jpn.* **69** (2000) Suppl. B. pp. 155.
- 14) T. Nomura and K. Yamada: *J. Phys. Soc. Jpn.* **72** (2003) 2053.